




Hydro-abrasive erosion on coated Pelton runners: Partial calibration of the IEC model based on measurements in HPP Fieschertal

Conference Paper

Author(s):

Felix, David ; Abgottspon, André; Albayrak, Ismail ; Boes, Robert 

Publication date:

2016-11

Permanent link:

<https://doi.org/10.3929/ethz-b-000125452>

Rights / license:

Creative Commons Attribution 3.0 Unported

Originally published in:

IOP Conference Series: Earth and Environmental Science 49(12), <https://doi.org/10.1088/1755-1315/49/12/122009>

Hydro-abrasive erosion on coated Pelton runners: Partial calibration of the IEC model based on measurements in HPP Fieschertal

D Felix¹, A Abgottspon², I Albayrak¹ and R M Boes¹

¹ Laboratory of Hydraulics, Hydrology and Glaciology (VAW), ETH Zürich, Hönggerberggring 26, CH-8093 Zurich, Switzerland

² Competence Center for Fluid Mechanics and Hydro Machines (CC FMHM), Hochschule Luzern (HSLU), Technikumstrasse 21, CH-6048 Horw, Switzerland

felix@vaw.baug.ethz.ch

Abstract. At medium- and high-head hydropower plants (HPPs) on sediment-laden rivers, hydro-abrasive erosion on hydraulic turbines is a major economic issue. For optimization of such HPPs, there is an interest in equations to predict erosion depths. Such a semi-empirical equation suitable for engineering practice is proposed in the relevant guideline of the International Electrotechnical Commission (IEC 62364). However, for Pelton turbines no numerical values of the model's calibration parameters have been available yet.

In the scope of a research project at the high-head HPP Fieschertal, Switzerland, the particle load and the erosion on the buckets of two hard-coated 32 MW-Pelton runners have been measured since 2012. Based on three years of field data, the numerical values of a group of calibration parameters of the IEC erosion model were determined for five application cases: (i) reduction of splitter height, (ii) increase of splitter width and (iii) increase of cut-out depth due to erosion of mainly base material, as well as erosion of coating on (iv) the splitter crests and (v) inside the buckets. Further laboratory and field investigations are recommended to quantify the effects of individual parameters as well as to improve, generalize and validate erosion models for uncoated and coated Pelton turbines.

1. Introduction

At medium- and high-head hydropower plants (HPPs) operated on sediment-laden rivers, turbine parts are subject to hydro-abrasive erosion. This causes high maintenance costs, and reduces turbine efficiency, electricity generation and revenues. As a basis for adequate countermeasures and optimizations in the design, operation and maintenance of such HPPs, the knowledge on hydro-abrasive erosion and its consequences needs to be improved. To this end, the Laboratory of Hydraulics, Hydrology and Glaciology (VAW) of ETH Zürich and the Competence Center for Fluid Mechanics and Hydro Machines (CC FMHM) of Hochschule Luzern, Switzerland, initiated an interdisciplinary research project.

In this project, sediment load, erosion on Pelton turbine runners and turbine efficiency changes have been measured and analyzed since 2012 at the high-head HPP Fieschertal in Valais, Switzerland. This run-of-river HPP with a design discharge of 15 m³/s and a gross head of 520 m is equipped with two horizontal 32 MW Pelton turbines [1]. The water used in this HPP originates from a glaciated



catchment and is known for relatively high suspended sediment concentration (SSC), i.e. $SSC = 0.5$ g/l on average, rising several times a year above 5 g/l. The injectors and the inner sides of the runner buckets are hard-coated with thermally sprayed tungsten carbide in a cobalt-chrome-matrix (WC-CoCr). The coating contributes to reduce the extent of erosion, but does not fully prevent the erosion of the base material. In each winter, damaged splitters and cut-outs are rounded by grinding if required and these zones are re-coated on-site. The Suspended Sediment Loads (SSL) and the so-called Particle Loads (PL) of the turbines in this HPP in the years 2012 to 2014 were quantified and presented in [2]. The turbine erosion in the corresponding period was also quantified and is treated in [3].

The present paper deals with the application of an equation to predict erosion depth, i.e. a semi-empirical erosion model, proposed by the relevant guideline of the International Electrotechnical Commission (IEC 62364, Edition 1, 2013) [4]. First, the processes causing hydro-abrasive erosion and the IEC model are described with focus on Pelton turbines. Then the model is applied to the data set of the HPP Fieschertal and the numerical values of a group of previously unknown model parameters are determined for five application cases to calibrate the model as far as possible. Finally, the results are discussed and recommendations on improvements of erosion prediction models for uncoated and coated Pelton turbines are given.

2. Hydro-abrasive erosion

2.1. Terminology and erosion mechanisms

Hydro-abrasion is a process causing material removal from a surface by the action of solid particles contained in flowing water (three-phase system). It is also described as a gradual alteration in state and shape of surfaces in contact with a particle-laden flow [5]. Hydro-abrasion is one of several processes causing erosion. In the field of hydro machines, also the combined terms ‘abrasive erosion’ [5] or ‘hydro-abrasive erosion’ are used [4]. The latter term is adopted in the present study.

Commonly, two erosion mechanisms are distinguished, mainly depending on the angle of attack α , i.e. the angle between the trajectories of the approaching particles and the surface (figure 1a) [6] [7]:

- Cutting of surface material due to sliding or impingement of particles at low α (‘cutting erosion’)
- Repeated plastic deformation of surface material and/or crack formation due to particle impacts at higher α , leading to breaking loose of material pieces (‘deformation erosion’)

For ductile materials, the erosion rate is usually highest between $\alpha \approx 20^\circ$ and 40° (figure 1b). For brittle materials however, the erosion rate is highest at $\alpha \approx 90^\circ$ and decreases pronouncedly with smaller α [6] [7]. While steel is typically ductile, hard-coatings (cermets) show brittle behaviour.

As a consequence of surface shape degradation due to hydro-abrasive erosion, cavitation may occur, which in turn may increase erosion (synergistic effect [4]). This complex interaction is not covered in the IEC erosion model [4] and is beyond the scope of the present study.

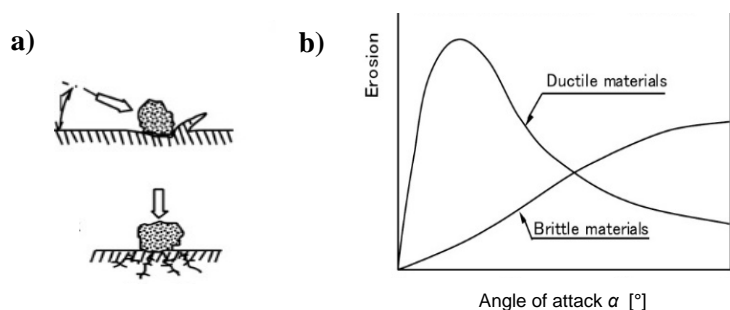


Figure 1.

Schematic representations of **a)** two erosion mechanisms and **b)** typical erosion rates as a function of the angle of attack α for ductile and brittle materials, respectively [8].

2.2. Typical conditions in Pelton turbines

In the turbine water of high-head HPPs, the mineral particles are typically smaller than 300 μm , because coarser particles are mostly excluded by upstream reservoirs or sand traps. Typically, most

particles are in the size range of silt (2 - 63 μm); particles in the size range of fine or medium sand are less frequent. The particles in the turbine water are generally transported in suspension and their velocity is similar to the flow velocity.

The highest velocities and accelerations occur in high-head Pelton turbines: for instance, at a head of 500 m, the relative velocity of the particle-laden flow in relation to turbine parts is 100 m/s at injectors (nozzles) and 50 m/s in a runner bucket. During the redirection of the flow in the two halves of a Pelton bucket for example, the acceleration normal to the bucket surface corresponds to typically several 10 000 times the gravitational acceleration. Such acceleration normal to the main flow direction drives particles generally outwards, leading to higher SSC close to convex surfaces, higher impingement rate and sliding of particles. The erosion inside Pelton buckets is due to the first mechanism mentioned above [9]. The second mechanism occurs typically on the splitter crests and the leading edges in the cut-outs, where α is high. These zones of Pelton buckets are particularly prone to erosion.

2.3. Erosion prediction

Many equations for the prediction of erosion have been developed since decades based on analytical considerations and laboratory tests, and numerical simulation methods have been increasingly used [10]. A major difficulty is to link the processes at the microscopic level to macroscopic models [11]. For engineering applications, there is an interest in easily applicable equations. Such semi-empirical equations comprise typically some calibration parameters and are limited to specific applications.

3. IEC erosion model for hydraulic turbines

3.1. Equation for the erosion rate

A working group of IEC formulated a concept for the modeling of hydro-abrasive erosion on hydraulic turbines for applied engineering purposes [12]. This concept and general design recommendations have been published in the IEC guideline 62364 [4]. It gives a factorized equation for the absolute erosion rate, considering the following parameters:

$$\frac{\Delta d_e}{\Delta t} = \frac{K_f}{RS^p} K_m w^x SSC k_{\text{size}} k_{\text{shape}} k_{\text{hardness}} \quad [\text{mm/h}] \quad (1)$$

where	Δt	Exposure period [h];
	Δd_e	Depth of erosion during Δt [mm];
	K_f	Coefficient reflecting the flow pattern, i.e. angle of attack and turbulence intensity [dimensions as resulting from calibration], intended to be constant for each turbine component, see note 1 below;
	RS	Reference size of a turbine [m]; for Francis turbines RS = runner diameter D , for Pelton turbines RS = inner bucket width B ;
	p	Exponent [-], a constant for each turbine component, for consideration of curvature-dependent effects, see note 1 below;
	K_m	Coefficient for the material at the surface of a turbine part [-], $K_m = 1$ for martensitic stainless steel with 13% Cr and 4% Ni; $K_m < 1$ for coating material;
	w	Characteristic relative velocity between the flow (or the particles) and the turbine part [m/s];
	x	Exponent [-], IEC suggests 3.4, literature values range between 2 and 4, see section 4.2.
	SSC	Suspended sediment mass concentration [g/l] = [kg/m ³], for Pelton $SSC = 0$ if no flow;
	k_{size}	Coefficient for particle size [-], IEC suggests to take the numerical value of d_{50} in [mm], d_{50} is the median size of graded particles which is not exceeded by 50% of the particle mass;
	k_{shape}	Coefficient for particle shape [-], IEC suggests $k_{\text{shape}} = 1$ for rounded or 2 for angular;
	k_{hardness}	Coefficient for particle hardness with respect to the hardness of the surface material [-], IEC suggest to take the mass fraction of particles harder than the surface material.

Note 1: Numerical values for K_f and p are given in IEC for five locations (parts) within uncoated Francis turbines. These values resulted from a statistical evaluation of field data of up to seven HPPs, mainly in China. For Pelton turbines, no such values are given in IEC due to scarcity of field data.

3.2. Integration over time and the concept of Particle Load (PL)

To obtain the erosion depth Δd_e over a time interval Δt , equation (1) is multiplied by Δt . The erosion depths in the time intervals since the start time t_0 until the time t are summed up to obtain the cumulated erosion depth $d_e(t)$ as follows:

$$d_e(t) = \frac{K_f}{RS^p} K_m w^x \underbrace{\sum_{i=1}^{(t-t_0)/\Delta t} SSC_i k_{size,i} k_{shape,i} k_{hardness,i}}_{= PL(t)} \Delta t \quad [\text{mm}] \quad (2)$$

The time step number is denoted as i . The parameters K_f , RS , p , K_m , w and x are constant or are assumed to be constant. The integral of the particle-related factors over the exposure period is called ‘particle load’ (PL). $PL(t)$ reflects the cumulated erosion potential of the particles passing through a turbine as a function of t since t_0 . PL has units of $[\text{h} \cdot \text{g/l}] = [\text{h} \cdot \text{kg/m}^3]$. In contrast to SSL , the PL is not a function of the discharge and does not depend on the turbine’s size. In equations (1) and (2), the erosion depth is modelled to be proportional to SSC and the exposure time. Thus, the same erosion depth is expected when a turbine runs e.g. for 1000 h at 0.5 g/l or for 100 h at 5 g/l (with the same particle properties), and the PL is the same in both cases.

3.3. Adaptation of the PL for Pelton runners

In contrast to reaction turbines or injectors of Pelton turbines, the erosion on a Pelton bucket takes place during only a part of the operation time (intermittent process). The erosion on a bucket decreases proportionally to the number of buckets z_2 because of the shorter exposure time per bucket. On the contrary, the erosion increases approximately proportional to the number of injectors (nozzles) z_0 because more buckets are simultaneously in contact with the sediment-laden water. The effects of z_0 and z_2 on the erosion rate or depth are stated in [13] (published in [14]) and are included in the so-called ‘reference model’ for Pelton turbines in the guideline [4]. To account for these effects, an adapted PL is introduced here:

$$PL \text{ for Pelton buckets} \quad PL_b = \frac{z_0}{z_2} PL \quad [\text{h} \cdot \text{g/l}] = [\text{h} \cdot \text{kg/m}^3] \quad (3)$$

The use of PL_b allows meaningful comparisons of the erosion potential on buckets between Pelton turbines with different numbers of nozzles and buckets.

4. Application and partial calibration of the IEC erosion model

4.1. Available erosion data and geometrical definitions

From the erosion measurements on the two machine groups (MGs) of the HPP Fieschertal, the following data are available from the years 2012 to 2014: (i) geometrical changes (in the range of mm) at the splitter crests and at the leading edges of the cut-outs of the runner buckets, where the coating was locally or systematically removed during sediment seasons with medium or high SSL (figure 2), and (ii) slight reductions of coating thicknesses (in the range of 10 μm) inside the buckets. The erosion on the nozzles was not monitored.

To quantify the erosion on the splitter crests and on the leading edges of the cut-outs, the geometrical definitions shown in figure 3 were introduced. The width s of an eroded splitter can easily be measured (e.g. with a ruler) if the splitter is flat on top and has sharp edges. The selected definition of s using the slopes of tangents [15] allows to determine s also if the splitter crest is unevenly eroded or rounded (e.g. due to grinding). The splitter width s is considered as an important indicator of the erosion status of a runner [16] [17]. The values of s and h are the maximum values along the splitter of a bucket. The cut-out depth d is the maximum value within the cut-outs of a bucket.

From the repeated measurements of these quantities at buckets no. 1 and 2 of each runner [3], the reduction of splitter height Δh , increase of splitter width Δs and increase of cut-out depth Δd were determined for each runner and each sediment season.

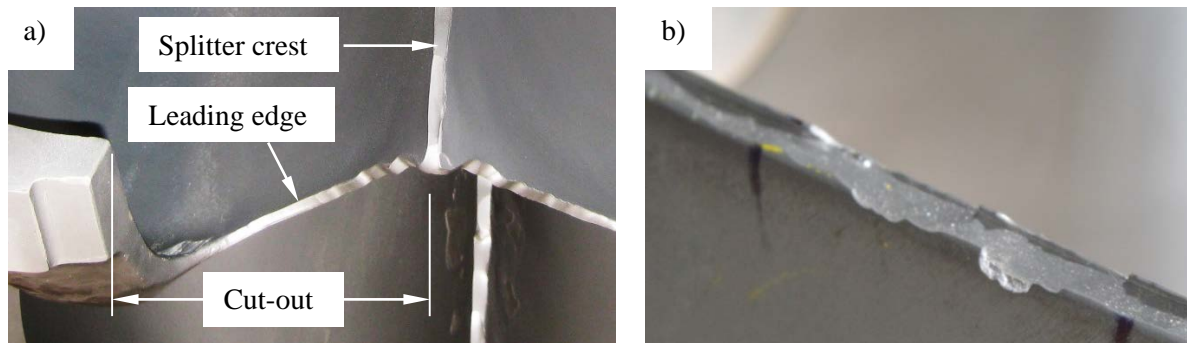


Figure 2. Examples of local erosion on hard-coated Pelton runners in the HPP Fieschertal: **a)** at splitter crests and leading edges of cut-outs (MG 2, August 08, 2012) and **b)** detail of eroded splitter with exposed base material on the crest (MG 2, November 15, 2013); the buckets were fully coated at the beginnings of the sediment seasons (pictures: VAW, ETH Zürich).

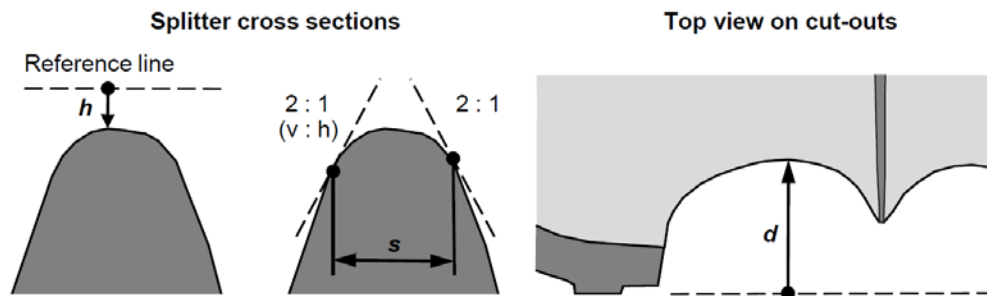


Figure 3. Geometrical definitions of h , s and d (modified from [15] and [3]).

4.2. Known values of model parameters

As a preparation for the application of the described erosion model, known parameter values are summarized in this section.

In Pelton turbines, the jet velocity and thus the relative velocity at the injector is $w_{inj} = (2gh_n)^{0.5}$ where h_n is the net head and g is the gravitational acceleration. For the HPP Fieschertal, the net head varies between 499 and 515 m. With the time-averaged net head of 510 m, $w_{inj} \approx 100$ m/s. The relative velocity w between the jet and the buckets is half of the jet velocity, thus $w = 50$ m/s.

IEC suggests a velocity exponent of $x = 3.4$ without specifying the turbine type and indicates a range between 2 and 4. For Pelton splitters, $2.8 \leq x \leq 3$ was found in laboratory tests [18]. In the present study, $x = 3$ was adopted, corresponding to [13] and other studies. Thus $w^x = 125'000$ m³/s³.

Each turbine of HPP Fieschertal has two injectors ($z_0 = 2$) and each runner has 20 buckets ($z_2 = 20$) with an inner width $B = RS = 0.65$ m.

The $PL(t)$ for each turbine (MG) were determined based on the operating hours and the measured time series of the SSC and the median particle size d_{50} . To do so, k_{size} was determined as a function of the actual d_{50} , as described in the definition of the variables of equation (1). The coefficient k_{size} is a linear function of d_{50} with $k_{size} = 1$ at $d_{50} = 1000$ μ m. For HPP Fieschertal, the temporal average of the k_{size} -values during the three years was 0.033. The coefficients $k_{hardness} = 0.75$ and $k_{shape} = 2$ were assumed to be constant over time (properties of the catchment area) [2].

The PL obtained with k_{size} according to IEC used in the present paper are on temporal average 30 times smaller than the PL obtained with $k_{size} = 1$ also reported in [2]. This recalls that the definition of $k_{size} = f(d_{50})$ is important for the determination of the PL .

4.3. Identification of unknown parameters

For the application of equation (2) at Pelton buckets, PL was replaced by PL_b according to equation (3). For HPP Fieschertal, the PL_b -values are ten times smaller than the PL -values because of $z_0 / z_2 = 0.1$. The parameters d_e , w^x , PL_b and RS are known. K_m is known for the base material ($K_m = 1$ by definition), but is unknown for the coating. In order to obtain an equation applicable to erosion of coating and/or base material, K_m was treated as a generally unknown parameter. K_f and p are unknown. The equation was solved for the unknown parameters. This group of parameters was denoted as C :

$$\frac{K_f}{RS^p} K_m = \frac{d_e(t)}{w^x PL_b(t)} \quad \text{with } C = \frac{K_f}{RS^p} K_m \quad (\text{definition}) \quad (4)$$

$$\text{for HPP Fieschertal} \quad C = \frac{1}{125\,000} \frac{d_e(t)}{PL_b(t)} \quad [\text{mm} / (\text{h} \cdot \text{g/l} \cdot \text{m}^3/\text{s}^3)] \quad (5)$$

4.4. Model application cases

In the following, the erosion model in the form of equation (5) is applied to the following cases:

- i. Decrease of splitter height Δh
- ii. Increase of splitter width Δs
- iii. Increase of cut-out depth Δd
- iv. Decrease of coating thickness inside the buckets Δc
- v. Decrease of coating thickness on the splitter crests (Δh within the coating)

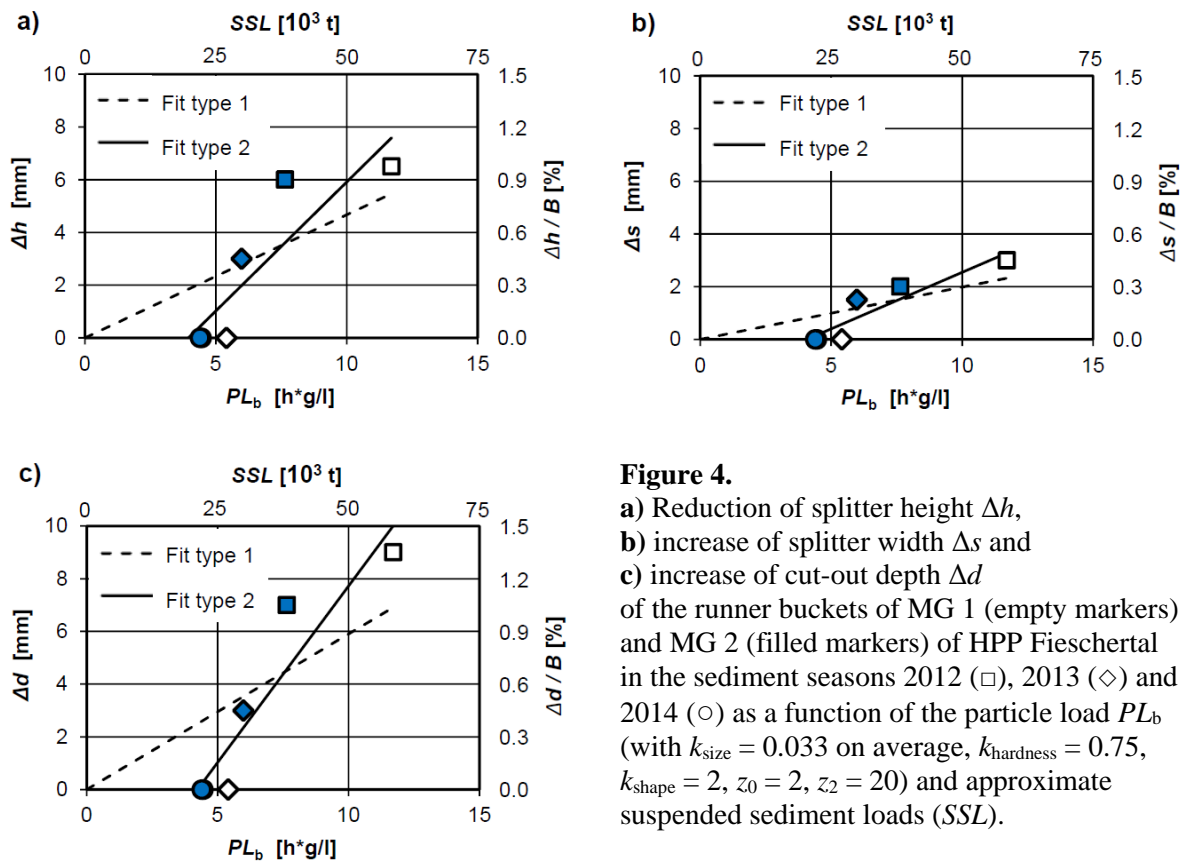
The IEC model was developed for the estimation of erosion depths on plane or moderately curved surfaces, as in case (iv). Applying such a model to geometrical changes at splitter crests or in cut-outs, as in the other four cases, corresponds to an extension of the original range of application, but is considered to be useful in practice. Δh , Δd and Δc are erosion depths because they are measured approximately in the directions of the erosion. However, Δs is not an erosion depth but a geometrical quantity depending on Δh , the cross-sectional shape of the splitter and the initial splitter width.

4.5. Geometrical changes due to erosion at splitters and cut-outs

The Δh , Δs and Δd obtained from the measurements are shown in figures 4a, b and c, respectively, as a function of the PL_b . Approximate SSL per turbine, as determined in [2], are also indicated on the top axes for comparison. It has been shown in [2] for the HPP Fieschertal that PL and SSL are approximately proportional over longer time spans such as at least one year. The absolute values of the geometrical changes are given on the left ordinates, whereas the relative geometrical changes (normalized with the inner bucket width $B = 0.65$ m) are given on the right ordinates of figures 4a, b and c. In 2014, the PL_b of both MGs were almost the same and no significant geometrical changes were measured (circular markers on top of each other). The data points in figures 4a, b and c show a similar pattern, indicating a systematic dependency of Δh , Δs and Δd on PL_b .

To determine the C -values in equation (5) for each of the three cases ($d_e = \Delta h$, Δs or Δd), linear least squares regressions were made on the data points shown in figure 4. In a first step, linear relations passing through the origins of the axes (denoted as ‘Fit type 1’) were selected, shown with dashed lines. The obtained C - and the R^2 -values are listed in the second column of table 1.

The investigated buckets were fully coated at the beginnings of the seasons (either factory coating or on-site re-coating). According to figure 4, the systematic erosion of base material at the splitter crests and the leading edges of the cut-outs began only after a certain PL_b . This threshold value was denoted as $PL_{b,0}$. The erosion process at the splitters and the leading edges of cut-outs can thus be divided in two stages: erosion of (1) mainly coating material and (2) mainly base material at a higher rate. According to unconstrained linear fits (denoted as ‘Fit type 2’, solid lines), the second stage of erosion began after $PL_{b,0} \approx 4.1$ [$\text{h} \cdot \text{g/l}$]. These lines fit significantly better to the data, i.e. the R^2 are higher than those of the constrained fits. The C -values resulting from the unconstrained fits are also listed in table 1. Note that these C -values refer to only the second stage of erosion, i.e. to $PL_{b,2} = PL_b - PL_{b,0}$. The C -value for Δs is less than half of that for Δh due to geometrical reasons (the flanks of the splitter are relatively steep). The C -values for Δd and Δh are similar.

**Figure 4.**

a) Reduction of splitter height Δh ,
b) increase of splitter width Δs and
c) increase of cut-out depth Δd
of the runner buckets of MG 1 (empty markers) and MG 2 (filled markers) of HPP Fieschertal in the sediment seasons 2012 (\square), 2013 (\diamond) and 2014 (\circ) as a function of the particle load PL_b (with $k_{size} = 0.033$ on average, $k_{hardness} = 0.75$, $k_{shape} = 2$, $z_0 = 2$, $z_2 = 20$) and approximate suspended sediment loads (SSL).

Table 1. Results of the fits between measured geometrical changes due to erosion and PL_b on Pelton buckets of HPP Fieschertal in the years 2012 to 2014; C and PL_b are defined in equations (4) and (3).

Application case (location in the Pelton bucket and measurement direction)	Erosion of coating and base material: Fit type 1 (dashed lines)		Distinguishing two stages of erosion (coating vs. base material): Fit type 2 (solid lines)	
	C		$PL_{b,0}$	C
	[mm / (h · g/l · m ³ /s ³)]		[h · g/l]	[mm / (h · g/l · m ³ /s ³)]
Reduction of splitter height Δh	$3.7 \cdot 10^{-6}$ ($R^2 = 0.54$)		4.0	$7.8 \cdot 10^{-6}$ ($R^2 = 0.78$)
Increase in splitter width Δs	$1.6 \cdot 10^{-6}$ ($R^2 = 0.58$)		4.1	$3.4 \cdot 10^{-6}$ ($R^2 = 0.86$)
Increase in cut-out depth Δd	$4.7 \cdot 10^{-6}$ ($R^2 = 0.56$)		4.2	$10.7 \cdot 10^{-6}$ ($R^2 = 0.87$)

4.6. Erosion of the coating in the buckets

In contrast to the three previous application cases, the following two cases deal with the erosion of coating material only. The hardness of WC-CoCr-coatings (approx. 1200 HV) is similar to that of quartz (Mohs' hardness 7). In the water of HPP Fieschertal, no minerals harder than quartz were detected. According to the definition of the parameters in equation (1), this would lead to $k_{hardness} = 0$ with respect to the coating and thus $PL_b = 0$. In order to keep non-zero PL_b -values and for comparability, the value of $k_{hardness} = 0.75$ (determined with respect to the base material) was also used in cases with erosion of the coating material.

Regarding erosion of coating in the buckets, two data points are available from the detailed template-based measurements before and after the sediment seasons initiated in spring 2013: the coating thickness in the buckets of MG 1 was reduced by 10 μm and 4 μm in the sediment seasons 2013 and 2014,

respectively [3]. These are average values over the surfaces inside buckets no. 1 and 2. With an uncertainty of $\pm 5 \mu\text{m}$, the coating thickness reduction measured in 2014 lies within the band of uncertainty. From these two data points, the following approximate C -value was obtained:

$$\text{Erosion of coating in buckets} \quad C \approx 1 \cdot 10^{-8} [\text{mm} / (\text{h} \cdot \text{g/l} \cdot \text{m}^3/\text{s}^3)]$$

It should be noted that this value has a higher relative uncertainty than the C -values in section 4.5. However, the higher relative uncertainty is of no concern for practical application, because the erosion of the coating in the buckets in two years without a major flood was small and is not decisive for the times between overhauls.

4.7. Erosion of the coating on the splitter crests

The analysis in section 4.5 showed that the coating on the splitter crests was systematically eroded after a $PL_{b,0} \approx 4.1 [\text{h} \cdot \text{g/l}]$. Note that this value is based on $k_{\text{hardness}} = 0.75$, as explained in the previous section. With the coating thickness meter used in this study [3], it was not possible to measure the coating thicknesses on the splitter crests for geometrical reasons. Assuming an initial coating thickness of 300 to 500 μm and a homogeneous and linear erosion on the splitter crest, the following approximate C -value results:

$$\text{Erosion of coating on splitter crests} \quad C \approx (0.6 \text{ to } 1) \cdot 10^{-6} [\text{mm} / (\text{h} \cdot \text{g/l} \cdot \text{m}^3/\text{s}^3)]$$

The C -value and the erosion rate of the coating on the splitter crests are thus about 60 to 100 times higher than in the buckets. This is mainly attributed to the effect of the angle of attack α on the erosion rate of brittle material, i.e. higher erosion at high α (figure 1).

5. Discussion

5.1. C -values

Various C -values were determined in the previous subsections for five different cases. C involves the parameters K_f , RS^p and K_m (equation 5). In the following, it is discussed whether it is possible to determine the values of some of these parameters based on the presented data set.

RS is known (0.65 m), but p is unknown. During the second stage of erosion, i.e. erosion of mainly base material, the coefficient for the properties of the eroded material is known by definition, $K_m = 1$. Thus, the values of the ratio K_f / RS^p are known for the cases (i) to (iii) during the erosion of the base material. From the presented data set, the exponent p , i.e. the effect of the turbine reference size RS on the erosion cannot be determined, because runners with only one size have been investigated.

Assuming that Δh , Δs and Δd do not significantly depend on RS , i.e. $p \approx 0$ and thus $RS^p \approx 1$, the K_f -values for the erosion of the base material correspond to the obtained C -values in the last column of table 1. Further measurements are required to investigate whether the slight difference in K_f for Δh and Δd is systematic (e.g. due to effects of the flow patterns and the profile shapes) or random, i.e. lies within the band of uncertainty.

The comparison of the C -values for erosion on the splitter crests in the base material (Δh in the second stage of erosion, $7.8 \cdot 10^{-6}$, table 1) and in the coating material (≈ 0.6 to $1 \cdot 10^{-6}$ in the same units) shows that the K_m -value for the coating is lower than that of the base material, as expected. The factor between the C -values of these two cases (both with high α) is about 10 (with the same k_{hardness} -values for both erosion of the coating and the base material).

Further measurements on buckets differing in size and with/without coating are required to further investigate the values of p , K_m and K_f for various cases.

5.2. Erosion of the coating in the buckets

During the years 2013 and 2014, the area-averaged erosion depths of the coating in the buckets (4 μm and 10 μm) were small compared to the initial coating thicknesses of 300 μm to 500 μm , and the erosion of coating material in the buckets was of no concern in these years.

In 2012 however, considerably more coating material was eroded in the buckets of the runner in MG 2: in the bottom region of some buckets, towards the bucket root, the coating was completely removed. In the vicinity of these zones, coating thicknesses of 50 μm to 100 μm were measured when the runner was taken out of operation after the major flood of July 2012 [3]. In the buckets of the runner in MG 1, however, no zones with totally eroded coating were observed after the major flood event, and the remaining coating thickness in the buckets was sufficient to use this runner for at least another three years. The considerable erosion inside the buckets of MG 2 in 2012 was probably related to the relatively wide and blunt splitters ($s = 8$ to 10 mm) which caused a disturbed flow field and could have induced cavitation as a secondary or combined damage mechanism. Local complete erosion of hard-coating in the bottom region of buckets was also observed in other studies [17].

6. Conclusions

The model for hydro-abrasive erosion proposed in the IEC guideline 62364 [4] with the concept of PL was summarized focusing on Pelton turbines. Based on sediment and erosion data acquired in the years 2012 to 2014 in the HPP Fieschertal, the numerical values C of a group of model calibration parameters were determined for five application cases: (i) reduction of splitter height Δh , (ii) increase of splitter width Δs , and (iii) increase of cut-out depth Δd mainly due to erosion of base material, as well as erosion of coating (iv) on the splitter crests and (v) inside the buckets.

Two stages of erosion at splitters and cut-outs were distinguished: Firstly the erosion of mainly coating, and secondly the erosion of mainly base material at a higher rate. The PL until the beginning of the second stage was quantified. C -values for Δh , Δs and Δd in the second stage were obtained from unconstrained linear fits. The C -values for the erosion of the coating on the splitters and inside the buckets confirm that the coating material has a much higher resistance to erosion than the base material. In particular, the C -value for the erosion of coating in the buckets is very low, proving that the coating is highly resistant to solid particle erosion if the angle of attack is low and there is no cavitation.

In field investigations, the parameters cannot be varied individually and systematically, and erosion depths cannot be measured frequently at most HPPs. The present study is based on three years of measurements in one HPP, i.e. the data set is limited and refers to a single bucket width (turbine size). Thus, it is not possible to determine the value of each model calibration parameter. However, with the definition of the C -value, it was possible to partly calibrate the erosion model and making it applicable. Care should be taken when applying the determined C -values to other HPPs, since the effects of some parameters have not been investigated yet, and the range of validity and the uncertainty of the calculated erosion depths are not yet quantified.

7. Outlook

In the described model, the factors k_{size} , K_f and p are the most challenging to quantify since they depend on many factors such as turbine type, location inside the turbine, flow pattern, angle of attack, radius of curvature and others. Further investigations by means of analytical considerations, laboratory tests, comprehensive measurements at further HPPs and numerical simulations are recommended. Additional laboratory and field data are required to (i) enlarge the data base especially for Pelton turbines, (ii) calibrate and validate semi-empirical equations and numerical models, (iii) extend and demonstrate the application range, and (iv) quantify the uncertainty of such models. For the further development of erosion models for uncoated and coated Pelton runners it is recommended to:

- Investigate the erosion processes of both the coating and the base material;
- Extend the models to four material phases: water, solid particles, base material and coating;
- Investigate the effect of turbine reference size (RS^p) and particle size (k_{size}) on erosion;
- Consider the effect of initial splitter width, in particular with respect to secondary damages;
- Investigate and consider non-linear effects in damage progression.

Acknowledgements

The support of the mentioned research project by swisselectric research, the Swiss Federal Office of Energy (SFOE), the HPP operator Gommerkraftwerke AG as well as the Swiss Competence Center for Energy Research - Supply of Electricity (SCCER-SoE) and the Research Fund of the Swiss Committee on Dams are gratefully acknowledged. Further thanks go to Endress+Hauser, Sigrist Photometers and Rittmeyer for lending measuring equipment as well as to all members of the project team for their contributions.

References

- [1] Felix D, Albayrak I, Abgottspon A and Boes R M 2016. Real-time measurements of suspended sediment concentration and particle size using five techniques. *Proc. 28th IAHR Symposium on Hydraulic Machinery and Systems, Grenoble, France, IOP Conf. Series*
- [2] Felix D, Albayrak I, Abgottspon A and Boes R M 2016. Suspended sediment measurements and calculation of the particle load at HPP Fieschertal. *Proc. 28th IAHR Symposium on Hydraulic Machinery and Systems, Grenoble, France, IOP Conf. Series*
- [3] Abgottspon A, Staubli T and Felix D 2016. Erosion of Pelton buckets and changes in turbine efficiency measured in the HPP Fieschertal. *Proc. 28th IAHR Symposium on Hydraulic Machinery and Systems, Grenoble, France, IOP Conf. Series*
- [4] IEC 62364 2013. Guide for dealing with hydro-abrasive erosion in Kaplan, Francis, and Pelton turbines. Edition 1.0, *International Electrotechnical Commission* (IEC) Geneva, Switzerland
- [5] Duan C G and Karelin V Y (eds.) 2002. Abrasive Erosion & Corrosion of Hydraulic Machinery, *Book series on Hydraulic machinery*, Vol. 2. London: Imperial College Press
- [6] Finnie I 1960. Erosion of surfaces by solid particles. *Wear* 1960(3): 87-103
- [7] Bitter J G A 1963. A study of erosion phenomena, parts I and II. *Wear* 1963(6): 5-21, 169-190
- [8] Matsumura M 2014. Erosion-Corrosion: An introduction to flow induced macro-cell corrosion. Bentham eBooks
- [9] Neopane H P, Dahlhaug O G and Cervantes M 2011. Sediment Erosion in Hydraulic Turbines. *Global J. of Researches in Engineering, Mechanical and Mechanics Engineering* 11(6)
- [10] Felix D, Albayrak I, Abgottspon A and Boes R M 2016. Hydro-abrasive erosion of hydraulic turbines caused by sediment – a century of research and development. *Proc. 28th IAHR Symposium on Hydraulic Machinery and Systems, Grenoble, France, IOP Conf. Series*
- [11] Meng H C and Ludema K C 1995. Wear models and predictive equations: their form and content. *Wear* 181-183: 443–457
- [12] Winkler K, Dekumbis R and Wedmark A 2010. Finding a way to estimate the amount of abrasion. *Proc. Hydro Conference, Lisbon, Portugal*
- [13] Sulzer Hydro 1996. Ein semi-empirisches Abrasionsmodell zur Vorhersage von hydro-abrasivem Verschleiss an X5 CrNi 13/4 Stahl (A semi-empirical abrasion model for the prediction of hydro-abrasive wear on X5 CrNi 13/4 steel). *Report STT.TB94.020* (in German)
- [14] DWA 2006. Entlandung von Stauräumen (Removal of reservoir sediments). Deutsche Vereinigung für Wasserwirtschaft, Abwasser und Abfall e.V., Hennef, Germany (in German)
- [15] Abgottspon A, Stern P, Staubli T, Felix D and Winkler K 2013. Measuring Turbine Abrasion and Efficiency Decrease: First Results of the Case Study at HPP Fieschertal. *Proc. Hydro Conference, Innsbruck, Austria: paper 18.05*
- [16] Boes R 2009. Real-time monitoring of SSC and PSD in the headwater way of a high-head hydropower plant. *Proc. 33rd IAHR Congress, Vancouver, Canada, 11026: 4037-4044*
- [17] Maltet R 2008. Pelton runner with high erosion caused by glacier sediment: assessment and measures. *Proc. 15th Intl. Seminar on HPPs, Doujak E (ed.), Vienna, Austria: 639-646*
- [18] Winkler K, Dekumbis R, Rentschler M, Parkinson E and Garcin H 2011. Understanding hydro-abrasive erosion. *Proc. Hydro Conference, Prague, Czech Republic*